PCCP

PAPER

View Article Online
View Journal

Cite this: DOI: 10.1039/d0cp02954h

Brushes and lamellar mesophases of comb-shaped (co)polymers: a self-consistent field theory

Ivan V. Mikhailov, [a] Ekaterina B. Zhulina [a] and Oleg V. Borisov *[ab]

Received 1st June 2020,
Accepted 14th September 2020

DOI: 10.1039/d0cp02954h

rsc.li/pccp

Theory describing equilibrium structural properties of solvent-free brushes formed by comblike polymers tethered by end segment of backbone to planar surface is developed using strong-stretching self-consistent field (SS-SCF) analytical approach and supported by numerical self-consistent field calculations based on the Scheutjens–Fleer (SF-SCF) method. The explicit dependence of self-consistent molecular potential on architectural parameters of comblike polymers is analyzed. It is demonstrated that distribution of local tension in backbones of long comblike polymers approaches that for linear chains. The star-to-comblike transition in solvent-free lamellas which occurs upon increase of backbone length of graft-polymer is analyzed.

1 Introduction

Brushes of branched polymers became a subject of intense theoretical investigation during the last decade.[1–7] Solvated or dry brushlike structures arise, *e.g.*, upon self-assembly of block copolymers with branched blocks in selective solvent[8–12] or in the melt state.[13–22]

An interest to covalently-linked to the surface or self-assembled brushes of branched macromolecules is motivated by possible applications in nanomedicine, particularly for drug and gene delivery systems[12] and antifouling surfaces[23–25] due to their architectural compatibility and increased number of potentially functionalized and exposed to the environment free ends. On the other hand, microphase segregated bulk morphologies of block copolymers comprising branched blocks exhibit unusual mechanical properties and are probed for design of novel biomimetic, including tissue-like materials.[26–29]

It was recently realized that structural properties of brushes formed by end-tethered polymers with specific branched architectures (*e.g.*, regular dendrons, arm-tethered stars, macrocycles, *etc.*) can be described by means of the analytical theory incorporating architecture-dependent self-consistent molecular potential. The pioneering study of Pickett[1] demonstrated a parabolic nature of the self-consistent molecular potential acting in brushes formed by strongly stretched root-tethered regular dendrons and paved the way to generalization of this analytical approach to other molecular architectures.[30–34] In our recent study[35] we applied the parabolic potential framework (SS-SCF) to study microphase segregated melts of diblock copolymers with comblike and/or bottlebrush blocks. The comblike and bottlebrush polymers were distinguished based on the conformational state of their backbones in melts. While comblike polymers with relatively loose grafts exhibit in melts the Gaussian statistics on all length scales, the densely grafted side chains in bottlebrush polymers lead to local stretching of their backbones. By using the asymptotic expressions for elasticity of graft-polymers with long backbones, we examined basic morphologies (spherical, cylindrical, and lamellar) of microphase segregated melt in the strong segregation limit. Under these conditions, the domains and matrix could be modelled as polymer brushes formed by the corresponding blocks of diblock copolymers.

In this paper we extend the analysis to brushes of comblike macromolecules with arbitrary length of backbones. By using the parabolic potential framework we examine how the elasticity and conformatons of comblike macromolecules in polymer brushes depend on the backbone degree of polymerization. Using these results we consider microphase segregated lamellas formed by symmetric diblock copolymers with equally branched blocks that can be assimilated to solvent-free polymer brushes. We analyze the "star-to-comb" transition invoked by increasing backbone length of the blocks. We demonstrate that in framework of SS-SCF approach, periodicity of lamellar mesophase demonstrates different power law dependences for diblock copolymers with short and long backbones, and prove the validity of conjecture used by us in the initial analysis of this transition.[35]

The rest of the paper is organized as follows. In Section 2 we formulate the model of the brush formed by comblike macromolecules and outline the analytical strong stretching self-consistent field (SS-SCF) approach. In Section 3 we discuss the predictions of the analytical theory for topological coefficient for such macromolecules, while in Section 4 discuss the distribution

[a] *Institute of Macromolecular Compounds of the Russian Academy of Sciences, St. Petersburg, Russia*
[b] *Institut des Sciences Analytiques et de Physico-Chimie pour l'Environnement et les Matériaux, UMR 5254 CNRS UPPA, Pau, France. E-mail: oleg.borisov@univ-pau.fr*

of elastic tension in the backbone and side chains in brushes of comblike polymers. In Section 5 we confront the predictions of the analytical theory to results of numerical modelling based on the Scheutjens–Fleer self-consistent field approach. In Section 6 we focus on star-to-comb transition in micro segregated lamella phase formed by symmetric copolymers with comblike blocks. In Section 7 we formulate the conclusions.

2 Brush of comblike macromolecules: model and SS-SCF formalism

Consider a graft homopolymer comprising P repeats each composed of the backbone spacer with degree of polymerization (DP) m and $q \geq 1$ side chains with n_j monomer units each ($j = 1, 2, \ldots, q$), linked to each junction on the backbone, see Fig. 1. The backbone and side chains are assumed to be chemically identical, and have monomer units with length l, volume υ, and Kuhn segment $b > l$. If $q > 1$, the macromolecules are termed "barbwire" polymers. The first backbone spacer attached to the surface (stem) has DP m_1. The last repeat unit can contain a different number $q_P \neq q$ of the side chains. The backbone has DP

$$M = m_1 + (P - 1)m \tag{1}$$

while the total degree of polymerization of the comblike macromolecule is

$$N = m_1 + (P-1)m + (P-1)\sum_{j=1}^{j=q} n_j + \sum_{p=1}^{p=q_P} n_p \tag{2}$$

The macromolecules are tethered to an impermeable planar surface with area s per chain. The grafting density $\sigma = 1/s$ ensures strong overlap of individual macromolecules so that the side chains and spacers are extended in the direction normal to the grafting surface with cut-off of polymer density profile (brush thickness) at distance $D = N\upsilon/s$ from the surface.

Following the strong stretching self-consistent field (SS-SCF) approach formulated earlier,[35] the molecular potential $U(z)$ in the solvent-free brush can be presented as

$$\frac{U(z)}{k_B T} = \frac{3}{2lb}\kappa^2\left(D^2 - z^2\right) \tag{3}$$

with architecture-dependent topological coefficient κ. The latter depends on DPs of the side chains (n_j), the backbone spacer (m), the stem (m_1), and the total number (P) of branching units but is remarkably independent of the chain grafting density σ or the brush geometry. Eqn (3) presumes the Gaussian (linear) elasticity of the tethered chains on all length scales. Crowding of the side chains near the branching points is not taken into account, which imposes a certain restriction on the branching activity, $q \gtrsim 1$. Another restriction on applicability of eqn (3) is appearance of the dead zones (depleted of the free ends of backbones), and the chains stratification for certain architectural parameters of comblike polymers. In these cases eqn (3) serves as an approximation to be examined by the numerical scf methods. The applicability of the parabolic potential approximation to any specific branched architecture of the brush-forming molecules can be checked by numerical self-consistent methods (*e.g.*, SF-SCF modelling[37]) that are also free of any preassumption about the mode of stretching and do account for finite extensibility of the macromolecules.

To eliminate the dependence of κ on DP N of the tethered polymer, we introduce the topological ratio

$$\eta = \frac{\kappa}{\kappa_{\text{linear}}} = \frac{2\kappa N}{\pi} \tag{4}$$

that specifies relative increase in the elastic free energy F per molecule in a brush of branched polymers with DP N, compared with the brush of linear macromolecules with same N. For linear chains,[36] $\kappa_{\text{linear}} = \pi/(2N)$, and in a solvent-free brush

$$F = \eta^2 F_{\text{linear}} \tag{5}$$

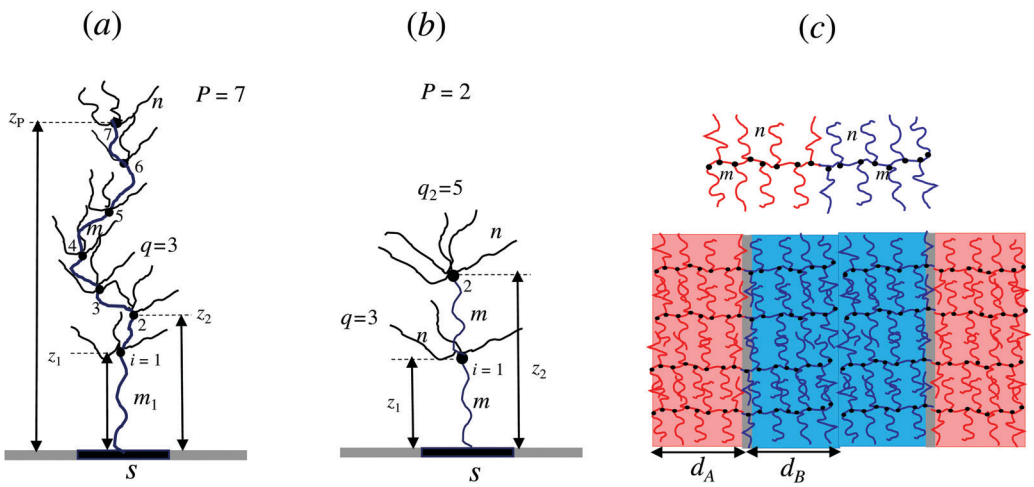

Fig. 1 Schematic of a comblike macromolecule with $P = 7$ (a) and $P = 2$ (b) branching points tethered to the surface by the root segment of the main chain and lamellar mesophase (c).

Notably, both κ and η do not depend on the brush geometry while F_{linear} does. Therefore knowledge of the elastic energy, F_{linear}, in brushes of linear chains, and of the topological ratio, $\eta = 2\kappa N/\pi$, allows for direct calculation of the elastic free energy F in the brushes of branched polymers. Because the elastic energy F_{linear} of linear chains ($\eta = 1$) in brushes with various geometries has been previously examined in the literature, we focus below on evaluation of the topological coefficient for comblike polymers with arbitrary number $P \geq 1$ of branching units.

3 Calculation of topological coefficient κ

A scheme to calculate the topological coefficient κ and topological ratio $\eta = 2\kappa N/\pi$ for a brush composed of comblike macromolecules is described in the Appendix 1. It is based on introduction of the chain trajectories and implements balancing of the elastic forces in all branching points of comblike polymer and conservation of DPs of all chain segments. Here, we present only basic equations for macromolecules with arbitrary number $P \geq 1$ of branching units (repeats of comblike polymer).

A set of linear recurrent equations for comblike polymer with $m_1 = m$ (see Fig. 1a),

$$\begin{aligned} &z_{i+1} - B(\kappa)\cdot z_i + z_{i-1} = 0 \quad i = 1, 2, ..., P-1 \\ &C(\kappa)\cdot z_P - z_{P-1} = 0 \quad i = P, \end{aligned} \tag{6}$$

with boundary condition $z_0 = 0$, and coefficients

$$B(\kappa) = \left[2\cos(\kappa m) - \sin(\kappa m)\cdot \sum_{j=1}^{j=q} \tan(\kappa n_j)\right] \tag{7}$$

$$C(\kappa) = \left[\cos(\kappa m) - \sin(\kappa m)\cdot \sum_{j=1}^{j=q_P} \tan(\kappa n_j)\right] \tag{8}$$

specifies vertical position z_i of branching unit i ($i = 2, 3, \ldots, P$) as a function of height z_1 of the first branching unit ($i = 1$), and the topological coefficient κ. As follows from eqn (6)–(8), all the details of molecular architecture (m,q,q_P,n_j) are incorporated in the expressions for $C(\kappa)$ and $B(\kappa)$.

Eqn (6) can be formulated in the matrix presentation as

$$\mathbf{A}_P\mathbf{Z}_P = \mathbf{0} \tag{9}$$

with $P \times P$ matrix $\mathbf{A}_P$ defined as

$$\mathbf{A}_P = \begin{pmatrix} -B(\kappa) & 1 & 0 & 0 & 0 & 0 \\ 1 & -B(\kappa) & 1 & 0 & 0 & 0 \\ 0 & 1 & -B(\kappa) & 1 & 0 & 0 \\ \cdots & \cdots & \cdots & \cdots & \cdots & \cdots \\ 0 & 0 & 0 & 1 & -B(\kappa) & 1 \\ 0 & 0 & 0 & 0 & -1 & C(\kappa) \end{pmatrix} \tag{10}$$

and column $\mathbf{Z}_P$ comprising positions z_i of the branching units ($i = 1, 2 \ldots P$),

$$\mathbf{Z}_P = \begin{pmatrix} z_1 \\ z_2 \\ z_3 \\ \cdots \\ z_{P-1} \\ z_P \end{pmatrix} \tag{11}$$

A nonzero solution of eqn (9) requires

$$\det \mathbf{A}_P = 0 \tag{12}$$

which provides an equation for the topological coefficient κ for comblike polymer with $P \geq 1$ of repeat units. The more general cases of $m_1 \neq m$ (Fig. 1b) and polydisperse side chains are considered in the Appendix 1.

Although the presented SS-SCF formalism provides a route to calculate the topological coefficient κ for comblike polymers with diverse architectural parameters, we focus below on a representative case of macromolecules with equal lengths of the side chains, $n_j = n$, and equal branching activity of all the branching points, $q_P = q$. These macromolecules have backbone DP

$$M = (m_1 - m) + Pm \tag{13}$$

and total DP

$$N = M + Pqn = (m_1 - m) + P(m + qn) = M\left[1 + qu + \frac{(w-1)}{P}\right] \tag{14}$$

with the notations

$$u = \frac{n}{m}; \quad w = \frac{m_1}{m} \tag{15}$$

In our previous publication[35] we presumed that the asymptotic dependence $\eta(u,q)$ for brushes of barbwire polymers with $P \to \infty$ is governed by the elasticity of their backbones. We used this conjecture to find η for a planar brush of comblike polymers. That is, in a planar brush with thickness $D = Nv/s$,

$$\frac{F_{\text{elastic}}}{k_B T} \simeq \frac{D^2}{lbM} = \frac{D^2}{lbN}\left[1 + qu + \frac{(w-1)}{P}\right]$$

to specify

$$\eta = \left[1 + qu + \frac{(w-1)}{P}\right]^{1/2} \approx (qu)^{1/2}, \quad qu \gg 1 \tag{16}$$

and

$$\kappa = \frac{\pi\eta}{2N} \approx \frac{\pi}{2M}(qu)^{-1/2}, \quad qu \gg 1 \tag{17}$$

As follows from eqn (16), for polymers with long backbones, $P \to \infty$, the topological ratio η is expected to depend only on the combination of parameters $qu = qn/m$. To check the conjecture we calculated the topological coefficient $\kappa(u,q,P)$ using

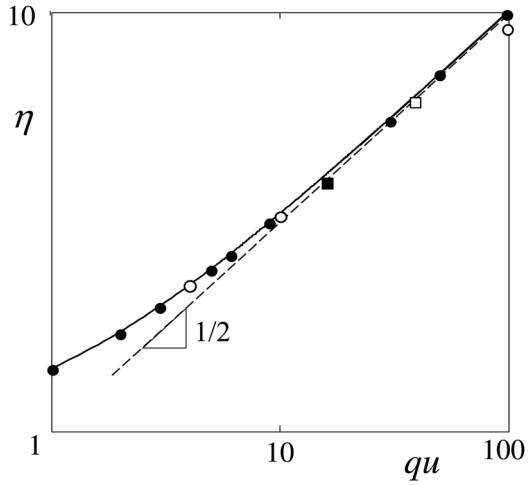

Fig. 2 Topological ratio $\eta(q,u)$ as function of qu for comblike polymer with $P = 22$, $m_1 = m$, in log–log coordinates. Asymptotic dependence $\eta = (1 + uq)^{1/2}$ is shown by black solid line. Black and white circles correspond to calculated values of $\eta(q,1)$ and $\eta(1,u)$ for various q and u values, $\eta(4,4) \approx \eta(1,16)$ and $\eta(4,10)$ indicated by black and white squares, respectively. Dashed line indicates slope 1/2.

eqn (12) for various sets of architectural parameters (u, q, and P) of barbwire polymers.

In Fig. 2 we present the topological ratio $\eta(q,u,P) = 2N\kappa(q,u,P)/\pi$, calculated *via* eqn (7), (8), (10) and (12) for barbwire polymers with long backbone, $P = 22$, $w = m_1/m = 1$, and various values of q and u as a function of product qu, in log–log coordinates. As seen in Fig. 2, the numerically calculated values of $\eta(q,1)$ (black circles), $\eta(1,u)$ (white circles), $\eta(4,4) \approx \eta(1,16)$ (indicated by single black square), and $\eta(4,10)$ (white square) all fall on the asymptotic dependence $\eta(q,u) = (1 + uq)^{1/2}$ (solid line, eqn (16)) with slope approaching 1/2 (dashed line) at $qu \simeq 10$. Therefore, the conjecture formulated in eqn (16) and (17) is clearly supported by the analytical calculations.

4 Conformations and elasticity of tethered comblike polymers

SS-SCF approach enables calculation of vertical positions (z_i) of the branching units ($i = 1, 2, \ldots, P - 1$) in the macromolecule with position z_P of its last branching unit as a function of reduced ranking number, i/P.

In Fig. 3 we present relative positions of the branching units, z_i/z_P, in barbwire macromolecules with $q = 4$, $u = n/m = 1$, and different numbers of repeats: $P = 2$ (indicated by black diamond with x-coordinate $i/P = 1/2$), $P = 5$ (triangles with x-coordinates $i/P = i/5$), and $P = 10$ (squares with x-coordinates $i/P = i/10$). Dashed solid line indicates relative height z_j/z_1 of monomer unit with ranking number j ($1 \le j \le m$) in the stem of starlike polymer ($P = 1$) with $q = 4$ free branches with the same DPs, as the stem as a function of j/m. Black solid line indicates the trajectory of a linear chain with DP M in the brush of similar chains. That is, relative position z_j/z_{end} of monomer unit with ranking number j in a linear chain with DP M and end-point position z_{end}, $z_j/z_{\mathrm{end}} = \sin(\pi j/2M)$, as a function of j/M. As seen in Fig. 3, an increase in P from $P = 1$ (starlike polymer with q free branches) to $P = 10$ makes the trajectory of the backbone almost indistinguishable from the trajectory of a linear chain with DP M and same end-point position.

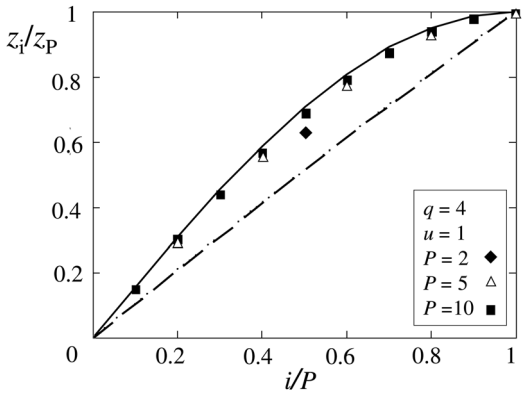

Fig. 3 Relative position z_i/z_P of the i-th branching point ($i = 0, 1, \ldots, P$) as a function of i/P for $u = 1$, $q = 4$, $P = 10$ (black squares), $P = 5$ (triangles), and $P = 2$ (black diamond); for $P = 1$ (star with $q = 4$ free branches) the trajectory is shown by dash-dotted line. Solid black curve shows the trajectory for the bare backbone ($q = 0$).

In Fig. 4 relative positions z_i/z_P of branching units are shown for conventional comblike polymer with $q = 1$, $P = 10$, $w = m_1/m = 1$, and values of $u = 1$ (white squares) and $u = 50$ (black squares). Black line indicates the trajectory of linear chain with DP M in the brush of similar chains. As seen in Fig. 4, an increase in $u = n/m$ from $u = 1$ to $u = 50$ leads to quite small deviations of the backbone trajectory from the trajectory of linear chain (black solid line).

In Fig. 5 we present reduced elastic forces, $G_{i,\uparrow}(z_i)/G_{\mathrm{ref}}(z_P)$ and $G_{i,\downarrow}(z_i)/G_{\mathrm{ref}}(z_P)$, acting at i-th branching unit up ($i = 0, 1, \ldots, P - 1$, filled symbols) and down ($i = 1, 2, \ldots, P$, empty symbols), respectively, as a function of its relative position, z_i/z_P (see Appendix 1 for details). $G_{\mathrm{ref}}(z_P) = 3z_P/lbM$ is the elastic tension

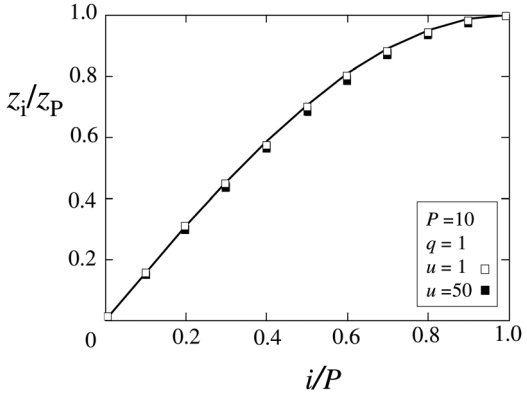

Fig. 4 Backbone trajectory: relative position of i-th branching point, z_i/z_P, ($i = 0, 1, \ldots, P$) as a function of i/P for comblike polymer with $P = 10$, $q = 1$, $w = 1$, $u = n/m = 1$ (white squares) and $u = 50$ (black squares). Solid line indicates relative position, $z_j/z_P = \sin(\pi j/2M)$, of j-th monomer in linear chain with DP M and end-point position z_P.

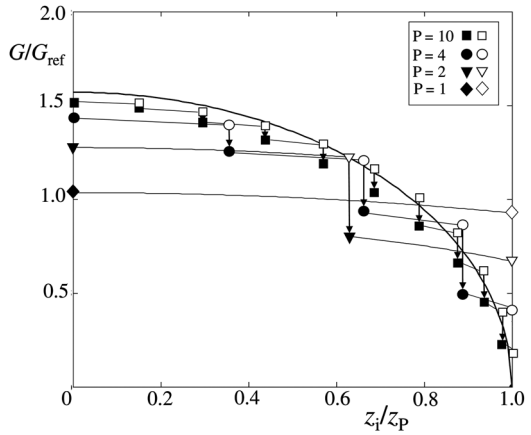

Fig. 5 Backbone contribution to reduced tension G/G_{ref} acting in branching point i up (solid symbols) and down (empty symbols) in the brush of combs with $m_1 = m$, $q = 4$, $u = n/m = 1$, and $P = 1, 2, 4, 10$. Here $G_{ref} = 3z_P/(lbM)$ is tension in uniformly stretched chain (backbone) with distance z_P between end-points. Black line indicates reduced tension in linear chain in the brush of backbones, eqn (19).

in a uniformly stretched linear chain with DP M and end-to-end distance z_P. Diamonds correspond to the stem of starlike polymer with $P = 1$, triangles, circles, and squares correspond to the backbones of comblike polymers with $P = 2$, 4, and 10, respectively, all with $u = n/m = 1$ and $q = 4$. Lines connecting symbols for neighboring branching units are the guide for eye, arrows indicate jumps between $G_{i,\downarrow}(z_i)$ (filled symbol) and $G_{i,\uparrow}(z_i)$ (empty symbol). The magnitudes of jumps between filled and empty symbols at each value of z_i/z_P specify the tension contributions of the side chains. Black line represents the reduced tension $G_{\text{linear}}(z)/G_{\text{ref}}(z_{\text{end}})$ in a linear chain with end-point position z_{end} in the brush of linear chains with DP M,

$$\frac{G_{\text{linear}}(z)}{G_{\text{ref}}(z_{\text{end}})} = \frac{\pi}{2}\sqrt{1-(z/z_{\text{end}})^2} \tag{18}$$

As seen in Fig. 5, the tension distribution in the backbone of macromolecule with number of repeats $P = 10$ closely reproduces the tension distribution in the linear chain ("bare" backbone). Further increase in P merely increases the number of jumps with progressively smaller magnitudes (not shown), indicating that contribution of the side chains in the backbone tension becomes almost negligible in the main part of the backbone. Only for few branching monomer units proximal to the backbone end-point, the cumulative tension imposed by the side chains is comparable to that in the backbone. It also follows from Fig. 5 that the reduced tension $G_{0,\uparrow}/G_{\text{ref}}(z_P)$ acting at the grafting surface ($z_0 = 0$) changes by the numerical prefactor on the order of unity (*i.e.*, from ≈ 1 to $\pi/2$) upon an increase in P from unity to infinity.

Similarity in conformations and elasticities of linear chains and backbones of long comblike polymers with $P \gg 1$ (Fig. 3–5) suggests that the distribution $g_M(z)$ of backbone end-points should be also similar to the distribution of the end-points in the brush of linear chains. In a planar solvent-free brush of linear chains with DP M, the distribution of the end-points is given by[36]

$$g(z_{\text{end}}) = \frac{1}{D}\frac{z_{\text{end}}}{\sqrt{D^2 - z_{\text{end}}^2}} \tag{19}$$

with $D = M\upsilon/s$. Assuming that eqn (19) holds for comblike polymers, *i.e.*,

$$g_{\text{comb}}(z_{\text{end}}) \approx \frac{1}{D}\frac{z_{\text{end}}}{\sqrt{D^2 - z_{\text{end}}^2}} \tag{20}$$

with brush thickness $D = N\upsilon/s$, and using the stretching function $E(z_{\text{end}}, z) = \frac{\pi}{2M}\sqrt{z_{\text{end}}^2 - z^2}$ for the backbone of comblike polymer, one predicts the average volume fraction $\varphi_M(z)$ of backbone monomer units,

$$\varphi_M(z) = \frac{\upsilon}{s}\int_z^D \frac{g_{\text{comb}}(z_{\text{end}})\mathrm{d}z_{\text{end}}}{E(z_{\text{end}}, z)} = \frac{M}{N} = \frac{1}{(1+qu)} \tag{21}$$

That is, the average volume fraction φ_M of the backbone monomers is predicted to be constant throughout the brush (except for conventional deviations in the presurface region and at the brush periphery).

5 SF-SCF numerical results

To verify the predictions of the analytical SS-SCF model formulated in the previous section, we performed numerical self-consistent field calculations using the Scheutjens–Fleer approach.[37] The numerical SCF method as analytical SS-SCF method is based on the mean-field approximation but it is free from the constraints imposed by the strong stretching approximation. This approach implements discrete lattice representation of the space. The lattice spacing equals a and it is assumed that $b=l=a$.

In Fig. 6 we present calculated profiles of the self-consistent potential $U(z)$ in solvent-free brushes with different sets of

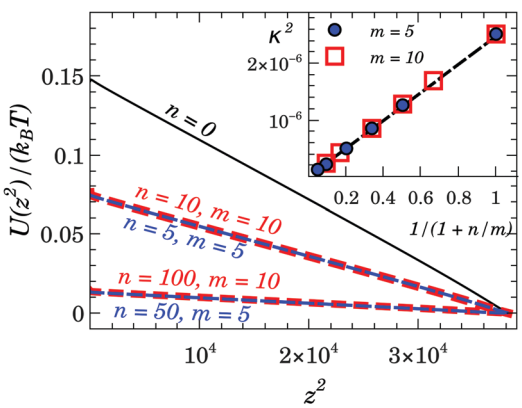

Fig. 6 Profiles of the self-consistent potential $U(z^2)$ in solvent-free brushes formed by linear chains with DP $M = 1001$ (solid line) or by molecular brushes with the same length of the main chain and different sets of n and m, as indicated at the curves. The thickness of the brush D is the same in all the cases. The insert demonstrated dependence of the topological coefficient κ calculated from the equation $U(z)/k_BT = (3/2a^2)\kappa^2(D^2 - z^2)$ as a function of $(1 + n/m)^{-1}$. Dashed line corresponds to asymptotic theoretical dependence $\kappa = (\pi/2M)(1 + n/m)^{-1/2}$.

parameters n and m (including brushes of linear chains, $n = 0$) but the same DP of the main chain $M = 1001$. In full agreement with eqn (3) self-consistent potential demonstrates linear decrease as a function of z^2 with a slope decreasing as a function of the ratio n/m. The insert in Fig. 6 demonstrates that topological coefficients κ calculated from the slopes of the $U(z^2)$ for different sets of n and m perfectly follow the asymptotic theoretical dependence

$$\kappa \approx \frac{\pi}{2M}\left(1+\frac{n}{m}\right)^{-1/2} \qquad (22)$$

which follows from eqn (3), (4) and (16) and applies for molecular brushes with long main chain.

As discussed above, the analytical SS-SCF approach predicted, that in the $P \gg 1$ limit, the conformations of the main chains of molecular brushes are similar to conformations of linear chains forming solvent-free brush. In particular, this refers to distribution of the free ends and distribution of elastic tension along main chains of the molecular brushes. This statement is well confirmed by the results of SF-SCF calculations: in Fig. 7 we present distribution of the free ends of the main chains for bottle-brushes with different sets of architectural parameters n and m and compare it to the theoretically predicted[36] distribution of free chain ends in the solvent-free brush of liner chains which is given by eqn (20).

The computed results perfectly match theoretical predictions. The identity of trajectories of the main chains of molecular brushes and linear chains in the brush is also confirmed by exact matching of distributions of (selected) branching points in the molecular brush and monomer units with the same ranking numbers in linear chains, as demonstrated by Fig. 8.

Finally, in Fig. 9 we present volume fraction profile $\varphi_M(z)$ for backbone monomer units which remain fairly constant inside the brush and match the dashed lines corresponding to predictions of eqn (21).

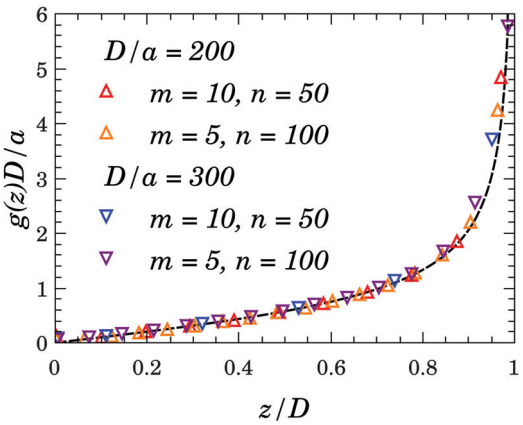

Fig. 7 Distribution of the end segment of the main chain of molecular brushes with $n = 50$, $m = 10$ and $n = 100$, $m = 5$, as indicated, at different values of D. $M = 1001$. Dashed line corresponds to theoretically predicted[36] distribution of the end segments in the dry brush formed by linear chains, eqn (20).

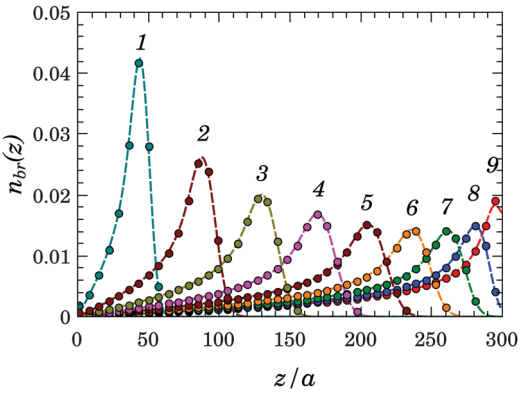

Fig. 8 Distribution of selected i-th monomer units of the main chain corresponding to branching points ($i = 100j$, $j = 1, 2, \ldots 9$ indicated at the curves) in the molecular brush with $M = 1001$, $n = 100$, $m = 5$. Dashed lines correspond to distribution of the monomer units with the same ranking numbers in a brush-forming linear chain with PD $M = 1001$.

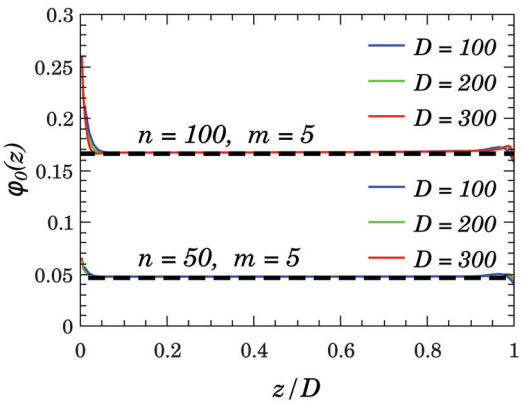

Fig. 9 Volume fraction profiles for the monomer units of the main chains in the brushes formed by molecular brushes with $M = 1001$, $n = 50$, $m = 10$ and $M = 1001$, $n = 100$, $m = 5$ at different values of the brush thickness D, as indicated in the figure. The dashed lines correspond to the fractions of monomer units in the brushes calculated as $(1 + n/m)^{-1}$.

6 Star-to-comb transition in lamellar mesophases

Microsegregation in melts of diblock AB copolymers with incompatible comb-like blocks leads to formation of regular domains of one component (A) in matrix of another (B). In the strong segregation limit, copolymers with equally long blocks A and B associate in planar lamellar layers (see Fig. 1c) in which junctions between the blocks are localized within narrow A/B interfaces. The blocks A and B in the corresponding layers can be envisioned as tethered to A/B interface, and thereby modelled as solvent-free brushes of comblike polymers. Planar solvent-free brushes of comblike polymers were considered in the previous section, and we use these results to describe lamellas formed by diblock AB copolymers with varying length of the backbones.

In our previous publication[35] we have analyzed the so-called star-to-comb transition in lamellas of microsegregated architecturally symmetric AB diblock copolymers with equally long

comblike blocks. In such macromolecules each block has backbone with DP $M = mP$, total DP $N = M(1 + u) = mP(1 + u)$, length l and volume υ of monomer unit in both, backbone and side chains, and Kuhn segment b. $P = 1$ corresponds to a linear chain with DP $N = m + n = m(1 + u)$.

The equilibrium grafting density $1/s$ of the macromolecules at A/B interfaces is found by balancing the elastic free energy, $F_A + F_B$, of the blocks and the free energy loss, $F_{A/B}$, at A/B interface. The latter is proportional to surface tension γ (surface free energy per area l^2, measured in units of thermal energy k_BT) times area s per chain, $F_{A/B}/k_BT = \gamma s/l^2$. Note that $F_A = F_B$ due to architectural similarity and equal DPs of the blocks, $N_A = N_B = N$.

The elasticity of comblike polymers, and their topological ratios η were analyzed in the previous sections of this paper. Eqn (5) enables to formulate the elastic free energy F_j of block j (j = A, B) as

$$\frac{F_j}{k_BT} = \eta^2\left(\frac{\pi^2}{8}\frac{d^2}{lbN}\right) = \eta^2\left(\frac{\pi^2}{8}\frac{N\upsilon^2}{lbs^2}\right), \quad j = A, B \tag{23}$$

Here, the term in brackets is the elastic free energy of linear chains with DP N in the solvent-free brush with thickness $d = N\upsilon/s$. By minimizing the free energy per molecule, $F_A + F_B + F_{A/B}$, with respect to area s, one finds the equilibrium grafting density $1/s$ of diblock copolymers on A/B interfaces, half thickness d of A and B lamellar layers,

$$d = \left(\frac{2\upsilon b}{\pi^2 l\gamma}\right)^{1/3}\left(\frac{N}{\eta}\right)^{2/3} \tag{24}$$

and periodicity of lamellar mesophase, $4d$. As follows from eqn (24), macromolecules with comblike blocks ($\eta > 1$) self-organize in lamellas with smaller periodicity compared to lamellas formed by linear diblock copolymers with same DP, N.

In our analysis[35] of the numerical SCFT calculations performed for copolymers with varying length M of backbone in architecturally symmetric comblike blocks,[38] we implemented a conjecture that the topological ratio η for brushes of comblike polymers with varying backbone length $M = mP$ exhibits two different asymptotic dependences, at $P \gtrsim 1$ (starlike) and $P \gg 1$ (comblike) limits. (In the latter case, η is given by eqn (16).) We now check the validity of this conjecture by calculating the topological ratio η *via* eqn (8), (12) and (10) for conventional comblike polymers with $q = 1$, $m/m_1 = 1$, and varied values of $u = n/m$ and P.

In Fig. 10 we present η as a function of $P = M/m$ for a set of comblike polymers with $u \in [1, 80]$ in log–log coordinates. Asymptotic values of $\eta = (1 + u)^{1/2}$ at $P \to \infty$ (eqn (16)) are shown by the horizontal lines with symbols indicating specific values of u, in the right part of the plot. As seen in Fig. 10, all SS-SCF data points are located to the right of the straight line $\eta = P$ (solid black line with slope 1). An increase in u up to 1000 (not shown in Fig. 10) confirms that $\eta(P)$ exhibits two asymptotic dependences:

$$\eta \approx \begin{cases} P, & P \ll u^{1/2} \quad \text{miktostar} \\ u^{1/2}, & P \gg u^{1/2} \quad \text{comb} \end{cases} \tag{25}$$

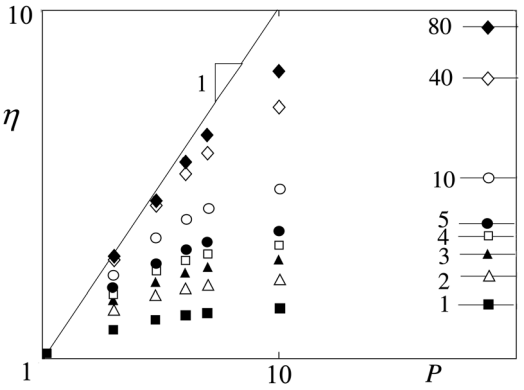

Fig. 10 Topological ratio η as a function of P, for comblike macromolecules with $m_1 = m$, $q = 1$ and $u = 1$ (filled squares), $u = 2$ (empty triangles), $u = 3$ (filled triangles), $u = 4$ (empty squares), $u = 5$ (filled circles), $u = 10$ (empty circles), $u = 40$ (empty diamonds), and $u = 80$ (filled diamonds), in log–log coordinates. Asymptotic values of $\eta = (1 + u)^{1/2}$ for $P = \infty$ are shown by horizontal lines in the right part of the plot, values of u are indicated. Asymptotic dependence $\eta = P$ is shown by straight solid line with slope 1.

The first line in eqn (25) corresponds to the starlike regime, when P long arms connected to a relatively short main chain are equally stretched and each of them contributes $\sim k_BTd^2/(Nlb/P)$ to the elastic free energy of a block. The second line in eqn (25) corresponds to the comblike regime and implies that the dominant contribution to the elastic free energy of a block is provided by extended main chain.

Therefore, half thickness d of alternating lamellar layers formed by each of the blocks with $u = n/m \gg 1$, demonstrates two asymptotic dependences corresponding to ''miktostar'' and comblike architectures of the macromolecule,

$$d \approx \left(\frac{2\upsilon b\gamma}{\pi^2 l}\right)^{1/3} \cdot \begin{cases} (N/P)^{2/3} \approx (mu)^{2/3} \approx n^{2/3}, & P \ll u^{1/2} \text{ miktostar} \\ M^{2/3}u^{1/3} \approx P^{2/3}n^{1/3}m^{1/3}, & P \gg u^{1/2} \text{ comb} \end{cases} \tag{26}$$

The transition between the two regimes, specified by intersection of two asymptotes in eqn (26), takes place at $P_* = u^{1/2} = (n/m)^{1/2}$, and the width of the transition region increases with u.

In Fig. 11 we compare periodicity ($4d$) of microsegregated lamellar phase formed by symmetric diblock coplymer with comblike blocks (with DP $N = M(1 + u) = mP(1 + u)$ each) to periodicity ($4d_0$) of microsegregated lamellar phase formed by symmetric diblock copolymer with DP $M = mP$ of each linear block. According to eqn (24) and (26), the numerical values of $Y = (4d)/(4d_0) = [(1 + u)/\eta]^{2/3}$ should be found between two asymptotic dependences,

$$Y = \begin{cases} [(1 + u)/P]^{2/3}, & P \ll u^{1/2} \\ (1 + u)^{1/3}, & P \gg u^{1/2} \end{cases} \tag{27}$$

In Fig. 11 ratio Y is presented as a function of P for various values of u in log–log coordinates with the same symbols as in Fig. 9. In all cases $Y(P) > 1$, rapidly decreases from $Y(1) = (1 + u)^{2/3}$ upon an increase in P, and approaches the value of $(1 + u)^{1/3}$ at $P \gg 1$. Asymptotic dependences in eqn (27) are shown for $u = 1$

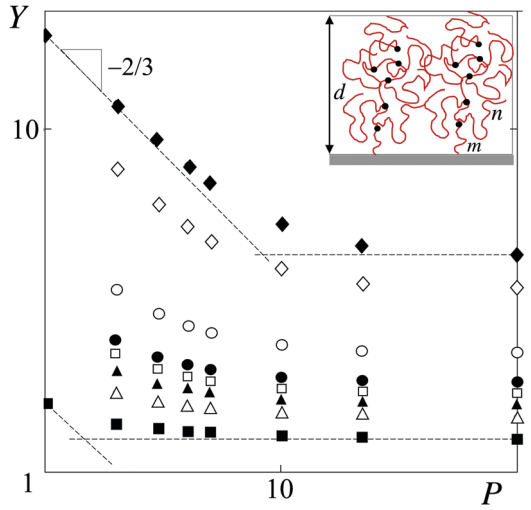

Fig. 11 Ratio $Y = (4d)/(4d_0)$ of period $4d$ of lamella mesophase formed by symmetric comblike copolymer AB with number of repeats P, $m_1 = m$, $q = 1$, $M = mP$, DP $N = M(1 + u)$ of each block, and varying $1 < u < 80$ (the same symbols as in Fig. 7), to period $4d_0$ in lamella mesophase formed by symmetric diblock copolymer with linear blocks with DP M each. Asymptotic dependences $Y = [(1 + u)/P]^{2/3}$ for $P \sim 1$ and $Y = (1 + u)^{1/3}$ for $P \gg 1$ are shown for $u = 1$ and $u = 80$ by dashed lines with slopes −2/3 and 0, respectively. Inset shows half of lamellar layer formed by comblike blocks A, black dots indicate branching units, A/B interface is marked grey.

and $u = 80$ by the dashed lines. For barbwire blocks with $q > 1$, eqn (24), (26), and (27) are modified as $u \to qu$.

Using similar arguments, eqn (24) can be extended to diblock copolymers with the same architectural parameters of the blocks (equal values of m, n, and P) but different l_j, υ_j, and b_j, as

$$d_A + d_B = \left(\frac{4\upsilon_A b_A \gamma}{\pi^2 l_A}\right)^{1/3} \frac{(1 + \upsilon_B/\upsilon_A)}{[1 + (l_A b_A \upsilon_B^2)/(l_B b_B \upsilon_A^2)]^{1/3}} \left(\frac{N}{\eta}\right)^{2/3} \quad (28)$$

to give periodicity of the lamellar phase, $2(d_A + d_B)$, with different prefactor compared to $4d$ (eqn (24)). However, because DP N and topological ratio η stay the same for both blocks, the transition point $P_* = u^{1/2}$ for copolymers with blocks having monomer units with different sizes (l_j,υ_j) and flexibilities (b_j) does not change.

However, an increase in branching activity $q > 1$ modifies the asymptotic dependences in eqn (25) as

$$\eta \approx \begin{cases} qP, & P \ll (u/q)^{1/2} \\ (qu)^{1/2}, & P \gg (u/q)^{1/2} \end{cases} \quad (29)$$

As a result, for barbwire diblock copolymers the transition point is shifted as $P_* = (u/q)^{1/2}$. That is, smaller length of backbone $M = mP$ is required to initiate star-to-comb transition in lamellas of diblock copolymers with architecturally symmetric barbwire blocks.

7 Conclusions

In this study we have theoretically examined the equilibrium properties of brushes formed by macromolecules with architectures ranging from starlike polymers to comblike (including barbwire) end-tethered to a planar surface. The applied analytical SS-SCF model presumed: (i) local flexibility of the side and main chains, (ii) the Gaussian elasticity of macromolecules on all length scales, and (iii) lack of brush vertical stratification.[30] These assumptions outline the regions of the parameter space in which the results of the analytical SS-SCF theory are justified. Comblike polymers with short stems, $m_1 \lesssim m$, can produce dead zones depleted of the free ends, particularly if $m_1/m \ll 1$ and number of periods P is relatively small. In this case, parabolic shape of molecular potential can serve as an approximation only. An increase in $P \gg 1$ decreases relative extension of the dead zone compared with the total brush thickness, H, and concomitant error in the elastic free energy F per molecule also decreases.

In the SS-SCF framework, branched macromolecules in the brush are exposed to the architecture-dependent molecular potential $U(z)$ which acts on the monomer units of the backbones and side chains. Compared with the scaling model of barbwire macromolecules[39] which accounts for local crowding of side chains near branching units, SS-SCF theory treats each side chain as stretched in the direction normal to the grafting surface according to the potential gradient, $\partial U(z)/\partial z$.

Because the parabolic potential gradient increases to the periphery of the brush, the side chains closer to the backbone end-point are stretched more than near the grafting surface. However, the total relative contribution of side chains to the backbone tension rapidly decreases with increasing number of repeats P in comblike macromolecules, and the conformations of the backbones become similar to those of linear polymers with DP M. The anticipated similarity between the distributions of end-points of linear chains and backbones of comblike polymers with $P \gg 1$ was confirmed by the numerical SF-SCF calculations. Based on this similarity, the average volume fraction $\varphi_M(z)$ of backbone monomer units was predicted to be constant throughout the brush, $\varphi_M(z) = M/N$, which was also corroborated by the numerical SF-SCF modelling.

The effects of side chains crowding, which is particularly important in the case of $q \gg 1$, cannot be strictly accounted for within presented here SS-SCF scheme based on the vertical force balance in each branching point. An approximate way to evaluate elastic free energy of bottlebrush molecules based on renormalization procedures presenting the bottlebrush molecule as an effective linear chain of superblobs, was described in ref. 35, 39 and 40. However, the accuracy of such approach is limited and, in contrast to SS-SCF scheme, it does not allow obtaining numerical factors. Also, attachment of multiple side chains to the same branching point unavoidable requires using of more bulky monomers units in the main chain. The effect of chemical difference between monomer units in the main and in the side chains can be accounted for within presented here scheme by incorporating different monomer unit size and Kuhn length upon calculating the elastic force balance in branching points.

Analysis of the topological ratio η for brushes composed of comblike polymers ($q = 1$) with varying backbone length M confirmed the existence of two power law asymptotes for the topological ratio: $\eta \approx P$ if $P \ll u^{1/2}$, and $\eta \approx u^{1/2}$ if $P \gg u^{1/2}$.

An increase in branching activity, $q > 1$, modifies these asymptotes for barbwire macromolecules as $\eta \approx qP$ if $P \ll (u/q)^{1/2}$, and $\eta \approx (qu)^{1/2}$ if $P \gg (u/q)^{1/2}$. These analytical results enabled a more accurate predictions for star-to-comb transition in microphase segregated lamellas formed by symmetric diblock copolymers with comblike and barbwire blocks.

In particular, the experimental and simulation data on lamellae formed by symmetric comblike diblocks are in accord with predictions of our model, as discussed in ref. 35. Our theory also predicts that an increase in number of side chains per monomer of *e.g.*, norbornene backbone in copolymer blocks should shift the star-to-comb transition in lamellae to smaller values of the backbone length $M \sim P$. This effect could be probed/checked experimentally.

Conflicts of interest

There are no conflicts to declare.

Appendix 1: calculation of topological coefficient κ for comblike polymers with arbitrary P

In this Appendix we present a route to calculate the topological coefficient κ for comblike macromolecules with arbitrary number P of repeats (see Fig. 1 in the main text) by using the conditions of force balance in every branching point, and the conservation of monomer units in each chain segment of the backbone between branching points and in each side chain.

Backbone stretching functions and tension for the case $m_1 = m$

We denote by z_i the vertical position of junction $i = 1, 2,\ldots,P$ above the surface (by definition $z_0 = 0$), and introduce the stretching functions, $E_i = \mathrm{d}z(j)/\mathrm{d}j$, of the spacer connecting junctions with ranking numbers $i-1$ and i as

$$E_i = \kappa\sqrt{\lambda_i^2 - z^2}, \quad i = 1, 2, \ldots, P \tag{30}$$

where λ_i is an unknown constant, and z is the distance from the grafting surface.

Conservation of spacer length between junctions $i-1$ and i,

$$\int_{z_{i-1}}^{z_i} \frac{\mathrm{d}z}{E_i} = m \tag{31}$$

relates constant λ_i to positions z_{i-1} and z_i of the respective junctions, $i-1$ and i, as

$$z_i = z_{i-1}\cos(\kappa m) + \sqrt{\lambda_i^2 - {z_{i-1}}^2}\sin(\kappa m), \quad i = 1, 2, \ldots, P \tag{32}$$

to give

$$\sqrt{\lambda_i^2 - {z_{i-1}}^2} = \frac{z_i - z_{i-1}\cos(\kappa m)}{\sin(\kappa m)} \tag{33}$$

Similarly, for junctions $i+1$ and i,

$$\sqrt{{\lambda_{i+1}}^2 - z_i^2} = \frac{z_{i+1} - z_i\cos(\kappa m)}{\sin(\kappa m)} \tag{34}$$

Using eqn (32)–(34) one can also calculate

$$\sqrt{\lambda_i^2 - z_i^2} = \frac{z_i\cos(\kappa m) - z_{i-1}}{\sin(\kappa m)} \tag{35}$$

We introduce the elastic forces $G_{i,\uparrow}$ and $G_{i,\downarrow}$ acting in the backbone at junction i up and down, respectively. In the linear elasticity regime, tension force $G(z)$ acting at height z in a chain segment is related to its stretching function $E(z)$ as

$$\frac{G(z)}{k_\mathrm{B}T} = \frac{3E(z)}{lb} \tag{36}$$

Tension force $G_{i,\uparrow}$ acting at junction $i = 0, 1,\ldots, P-1$ with coordinate z_i up is thereby given by

$$\begin{aligned}\frac{G_{i,\uparrow}(z_i)}{k_\mathrm{B}T} &= \frac{3E_{i+1}(z_i)}{lb} \\ &= \frac{3}{lb}\kappa\sqrt{{\lambda_{i+1}}^2 - z_i^2} \\ &= \frac{3}{lb}\kappa\frac{[z_{i+1} - z_i\cos(\kappa m)]}{\sin(\kappa m)}\end{aligned} \tag{37}$$

Tension force $G_{i,\downarrow}$ acting at junction $i = 1, 2,\ldots, P$ down is given by

$$\begin{aligned}\frac{G_{i,\downarrow}(z_i)}{k_\mathrm{B}T} &= \frac{3E_i(z_i)}{lb} \\ &= \frac{3}{lb}\kappa\sqrt{\lambda_i^2 - z_i^2} \\ &= \frac{3}{lb}\kappa\frac{[z_i\cos(\kappa m) - z_{i-1}]}{\sin(\kappa m)}\end{aligned} \tag{38}$$

The pulling force acting at the grafting surface ($z_0 = 0$) by the tethered macromolecule is given by

$$\frac{G_{0,\uparrow}(z_0)}{k_\mathrm{B}T} = \frac{3}{lb}\kappa\frac{z_1}{\sin(\kappa m)} \tag{39}$$

Tension contribution of side chains

In addition to backbone tensions $G_{i,\uparrow}$ and $G_{i,\downarrow}$, an additional vertical force $G_{i,s}$ acting at junction i in the z-direction is induced by the side chains. Because elastic tension at the free end of any side chain is zero, the stretching function E_{ij} of the side chain with ranking number j emanating from junction i is given by

$$E_{ij} = \kappa\sqrt{{z_{ij}}^2 - z^2} \tag{40}$$

where position z_{ij} of the end-point of side chain with DP n_j can be found from the condition

$$\int_{z_i}^{z_{ij}} \frac{\mathrm{d}z}{E_{ij}} = n_j \tag{41}$$

As a result, the stretching function E_{ij} of this side chain yields

$$E_{ij} = \kappa\sqrt{\frac{z_i^2}{\cos^2(\kappa n_j)} - z^2} \tag{42}$$

The latter expression ensures conservation of the side chain length (n_j), and zero tension at the side chain free end with height $z_{ij} = z_i/\cos(\kappa n_j)$. The total stretching force due to side chains acting up at junction with ranking number $i = 1, 2, \ldots, P$ is thereby given by

$$\frac{G_{i,s}}{k_B T} = \sum_{j=1}^{j=q} \frac{3E_{ij}(z_i)}{lb} = \frac{3\kappa}{lb} z_i \sum_{j=1}^{j=q} \tan(\kappa n_j) \tag{43}$$

In the case of side chains with equal length, $n_j = n$,

$$\frac{G_{i,s}}{\kappa_B T} = \frac{3\kappa}{a^2} z_i q \tan(\kappa n) \tag{44}$$

Similarly, the tension force due to side chains at the last junction ($i = P$) is

$$\frac{G_{P,s}}{k_B T} = \frac{3\kappa}{lb} z_P \sum_{j=1}^{j=q_P} \tan(\kappa n_j) \tag{45}$$

which in the case of $n_j = n$ reduces to

$$\frac{G_{P,s}}{k_B T} = \frac{3\kappa}{lb} z_P q_P \tan(\kappa n) \tag{46}$$

Balance of elastic forces acting at branching unit $i < P$ yields

$$G_{i,\uparrow} + G_{i,s} = G_{i,\downarrow} \tag{47}$$

or, equivalently,

$$\frac{3}{lb}\kappa\frac{z_{i+1} - z_i\cos(\kappa m)]}{\sin(\kappa m)} + \frac{3\kappa}{a^2} z_i \sum_{j=1}^{j=q} \tan(\kappa n_j) = \frac{3}{lb}\kappa\frac{[z_i\cos(\kappa m) - z_{i-1}]}{\sin(\kappa m)} \tag{48}$$

which provides the following relationship between vertical positions of three neighboring junctions,

$$z_{i+1} - z_i\left[2\cos(\kappa m) - \sin(\kappa m)\sum_{j=1}^{j=q}\tan(\kappa n_j)\right] + z_{i-1} = 0, \quad 1 \le i \le P-1 \tag{49}$$

The force balance at the last junction ($i = P$) is ensured by equality

$$G_{P,\downarrow} = G_{P,s} \tag{50}$$

which is equivalent to the following relationship

$$z_P\left[\cos(\kappa m) - \sin(\kappa m)\sum_{j=1}^{j=q}\tan(\kappa n_j)\right] - z_{P-1} = 0 \tag{51}$$

The set of recurrent equations

$$\begin{aligned} &z_{i+1} - B(\kappa)\cdot z_i + z_{i-1} = 0 \quad i = 1, 2, \ldots, P-1 \\ &C(\kappa)\cdot z_P - z_{P-1} = 0 \quad i = P \end{aligned} \tag{52}$$

with

$$B(\kappa) = \left[2\cos(\kappa m) - \sin(\kappa m)\cdot\sum_{j=1}^{j=q}\tan(\kappa n_j)\right], \tag{53}$$

$$C(\kappa) = \left[\cos(\kappa m) - \sin(\kappa m)\cdot\sum_{j=1}^{j=q_P}\tan(\kappa n_j)\right] \tag{54}$$

and the boundary condition $z_0 = 0$ can be formulated in matrix presentation as

$$\mathbf{A}_P\mathbf{Z}_P = 0 \tag{55}$$

Here, $P \times P$ matrix $\mathbf{A}_P$ is defined as

$$\mathbf{A}_P = \begin{pmatrix} -B(\kappa) & 1 & 0 & 0 & 0 & 0 \\ 1 & -B(\kappa) & 1 & 0 & 0 & 0 \\ 0 & 1 & \cdots & \cdots & 0 & 0 \\ 0 & 0 & \cdots & \cdots & 1 & 0 \\ 0 & 0 & 0 & 1 & -B(\kappa) & 1 \\ 0 & 0 & 0 & 0 & -1 & C(\kappa) \end{pmatrix} \tag{56}$$

and column $\mathbf{Z}_P$ is composed of vertical positions z_i of branching units,

$$\mathbf{Z}_P = \begin{pmatrix} z_1 \\ z_2 \\ z_3 \\ \cdots \\ z_{P-1} \\ z_P \end{pmatrix} \tag{57}$$

A non-zero solution of eqn (55) requires

$$\det\mathbf{A}_P = 0 \tag{58}$$

which provides the equation for topological coefficient κ. As it is seen from eqn (52) and (54), positions z_i of the branching units are calculated *via* the same scheme for macromolecules with various comblike architectures with all the details of molecular architecture (m,q,n_j) contained in the expressions for $C(\kappa)$ and $B(\kappa)$.

To illustrate the calculation scheme we consider two examples: (i) starlike polymer ($P = 1$) with polydisperse branches, and (ii) the shortest comblike macromolecule ($P = 2$) with $m = n$, and $q \ge 1$ side chains emanating from the first branching unit, and $q_P = q_2 \ne q$ free branches emanating from the second (last) branching unit, with n monomer units each (see Fig. 1b).

Starlike polymer with $P = 1$

In this case, matrix $\mathbf{A}_P$ reduces to a single element $C(\kappa)$ in eqn (54), $\mathbf{A}_1 = (C(\kappa))$, and eqn (58) leads to $C(\kappa) = 0$, or, equivalently,

$$\tan(\kappa m)\cdot\sum_{j=1}^{j=q_P}\tan(\kappa n_j) = 1 \tag{59}$$

For symmetric stars with q equally long free branches, $n_j = n$, and $m = n$, eqn (59) provides the known[30] result

$$\kappa = \frac{1}{n}\arctan\left(q^{-1/2}\right) \tag{60}$$

Comblike polymer with $P = 2$, $m = n$, $q_2 \neq q$

In this case, matrix $\mathbf{A}_P$ reduces to

$$\mathbf{A}_2 = \begin{pmatrix} -B(\kappa) & 1 \\ -1 & C(\kappa) \end{pmatrix} \tag{61}$$

with

$$B(\kappa) = [2\cos(\kappa n) - \sin(\kappa n)\cdot q\tan(\kappa n)] \tag{62}$$

$$C(\kappa) = [\cos(\kappa n) - \sin(\kappa n)\cdot q_2\tan(\kappa n)] \tag{63}$$

By applying eqn (52) for $P = 2$ and implementing $z_0 = 0$ for position of the tethered monomer, vertical positions z_1 and z_2 of the first and second branching points are related as $z_2/z_1 = B(\kappa)$, while eqn (58) for the topological coefficient κ reduces to

$$C(\kappa)\cdot B(\kappa) = 1 \tag{64}$$

By substituting expressions for $B(\kappa)$ and $C(\kappa)$ from eqn (63) and (62) in eqn (64), and using $\tan(\kappa n)$ as a variable, one finds an analytical solution of eqn (64),

$$\kappa = n^{-1}\arctan\left\{\sqrt{\frac{(2q_2+q+1) - \sqrt{(2q_2+q+1)^2 - 4qq_2}}{2qq_2}}\right\} \tag{65}$$

Eqn (58) enables numerical calculation of the topological coefficient κ for arbitrary values of P as a function of the architectural parameters of the macromolecules.

Force balance equations for the case $m_1 \neq m$

We now extend the previous calculation scheme to the case when the first (root) spacer has length $m_1 \neq m$. Clearly everything remains unchanged in eqn (52) for $i = 2, 3, \ldots, P$, that is

$$\begin{aligned} &z_{i+1} - B(\kappa)\cdot z_i + z_{i-1} = 0 \quad 2 \le i \le P-1 \\ &C(\kappa)\cdot z_P - z_{P-1} = 0 \quad i = P \end{aligned} \tag{66}$$

The elastic elongation of the first spacer (stem) is now specified by the stretching function

$$E_1 = \kappa\sqrt{\lambda_1^2 - z^2} = \kappa\sqrt{\frac{z_1^2}{\sin^2(\kappa m_1)} - z^2} \tag{67}$$

with $\lambda_1 = z_1/\sin(\kappa m_1)$ determined *via* conservation of length of the first spacer,

$$\int_{z_0}^{z_1}\frac{\mathrm{d}z}{E_1} = m_1 \tag{68}$$

Force balance in the first branching unit, $i = 1$, expressed as

$$E_2(z_1) + \kappa z_1 q\tan(\kappa n) = E_1(z_1) \tag{69}$$

leads (taking advantage of eqn (33) specifying $E_2(z_1)$, $i = 2$) to

$$\begin{aligned} \frac{z_2}{z_1} &= \left[\frac{\sin(\kappa m)}{\tan(\kappa m_1)} + \cos(\kappa m) - q\tan(\kappa n)\right] \\ &= B(\kappa) + \frac{\sin[\kappa(m-m_1)]}{\sin(\kappa m_1)} \equiv B_1(\kappa) \end{aligned} \tag{70}$$

Therefore in case of $m_1 \neq m$ the set of recurrent relations in eqn (66) is generalized as

$$\begin{aligned} &z_2 - B_1(\kappa)\cdot z_1 = 0 \quad i = 2 \\ &z_i - B(\kappa)\cdot z_{i-1} + z_{i-2} = 0 \quad i = 3, 4, \ldots, P-1 \\ &C(\kappa)\cdot z_P - z_{P-1} = 0 \quad i = P \end{aligned} \tag{71}$$

and matrix $\mathbf{A}_P$ in eqn (58) for the topological coefficient κ is modified as

$$\tilde{\mathbf{A}}_P = \begin{pmatrix} -B_1(\kappa) & 1 & 0 & 0 & 0 & 0 \\ 1 & -B(\kappa) & 1 & 0 & 0 & 0 \\ 0 & 1 & \cdots & \cdots & 0 & 0 \\ 0 & 0 & \cdots & \cdots & 1 & 0 \\ 0 & 0 & 0 & 1 & -B(\kappa) & 1 \\ 0 & 0 & 0 & 0 & -1 & C(\kappa) \end{pmatrix} \tag{72}$$

The topological coefficient κ is calculated in this case from the condition

$$\det\tilde{\mathbf{A}}_P = 0$$

Topological coefficient κ for comblike polymer with irregular grafting of side chains

If lengths m_i of the spacers between branching units, and of the side chains, n_{ij}, originating from branching unit i with branching activity q_i, vary in the comblike polymer, the topological coefficient κ can still be found from the conditions of local force balance in every branching unit,

$$G_{i,\uparrow} + G_{i,s} = G_{i,\downarrow} \tag{73}$$

and the conditions of length concervation in all side chains, eqn (41), and in all spacers,

$$\int_{z_{i-1}}^{z_i}\frac{\mathrm{d}z}{E_i} = m_i \tag{74}$$

The latter condition leads to

$$z_i = z_{i-1}\cos(\kappa m_i) + \sqrt{\lambda_i^2 - z_{i-1}^2}\sin(\kappa m_i), \quad i = 1, 2, \ldots, P \tag{75}$$

and

$$\sqrt{\lambda_i^2 - z_{i-1}^2} = \frac{z_i - z_{i-1}\cos(\kappa m_i)}{\sin(\kappa m_i)} \tag{76}$$

Similarly, for spacer $i + 1$

$$\sqrt{\lambda_{i+1}^2 - z_i^2} = \frac{z_{i+1} - z_i\cos(\kappa m_{i+1})}{\sin(\kappa m_{i+1})} \tag{77}$$

and

$$\sqrt{\lambda_i^2 - z_i^2} = \frac{z_i \cos(\kappa m_i) - z_{i-1}}{\sin(\kappa m_i)} \tag{78}$$

Elastic forces $G_{i,\uparrow}(z_i)$, $G_{i,\downarrow}(z_i)$, and $G_{i,s}(z_i)$ acting at branching point $i < P$ are now given by

$$\begin{aligned}\frac{G_{i,\uparrow}(z_i)}{k_B T} &= \frac{3E_{i+1}(z_i)}{lb} \\ &= \frac{3}{lb}\kappa\sqrt{\lambda_{i+1}^2 - z_i^2} \\ &= \frac{3}{lb}\kappa\frac{[z_{i+1} - z_i\cos(\kappa m_{i+1})]}{\sin(\kappa m_{i+1})}\end{aligned} \tag{79}$$

$$\begin{aligned}\frac{G_{i,\downarrow}(z_i)}{k_B T} &= \frac{3E_i(z_i)}{lb} \\ &= \frac{3}{lb}\kappa\sqrt{\lambda_i^2 - z_i^2} \\ &= \frac{3}{lb}\kappa\frac{[z_i\cos(\kappa m_i) - z_{i-1}]}{\sin(\kappa m_i)}\end{aligned} \tag{80}$$

$$\begin{aligned}\frac{G_{i,s}}{k_B T} &= \sum_{j=1}^{j=q_i}\frac{3E_{i,p}(z_i)}{lb} \\ &= \frac{3\kappa}{lb}z_i\sum_{j=1}^{j=q_i}\tan(\kappa n_{ij})\end{aligned} \tag{81}$$

Balance of forces yields

$$\begin{aligned}&z_{i+1} - B_i(\kappa)\cdot z_i + D_{i-1}(\kappa)\cdot z_{i-1} = 0 \quad i = 1, 2, \ldots, P-1 \\ &C_P(\kappa)\cdot z_P - z_{P-1} = 0 \quad i = P\end{aligned} \tag{82}$$

with

$$\begin{aligned}B_i(\kappa) &= \cos(km_{i+1}) + \frac{\sin(km_{i+1})}{\tan(km_i)} \\ &\quad - \sin(km_{i+1})\sum_{j=1}^{q_i}\tan(\kappa n_{ij}), \quad i = 1, 2, \ldots, P-1\end{aligned} \tag{83}$$

the newly introduced parameter

$$D_{i-1}(\kappa) = \frac{\sin(km_{i+1})}{\sin(km_i)}, \quad i = 2, 3, \ldots P-1 \tag{84}$$

and

$$C_P = \cos(\kappa m_P) - \sin(\kappa m_P)\sum_{j=1}^{q_P}\tan(\kappa n_{P_j}) \tag{85}$$

As a result, matrix $\tilde{\mathbf{A}}_P$ is modified as $\tilde{\mathbf{A}}_P \rightarrow \hat{\mathbf{A}}_P$ with

$$\hat{\mathbf{A}}_P = \begin{pmatrix} -B_1(\kappa) & 1 & 0 & 0 & 0 & 0 \\ D_1(\kappa) & -B_2(\kappa) & 1 & 0 & 0 & 0 \\ 0 & D_2(\kappa) & -B_3(\kappa) & \cdots & 0 & 0 \\ 0 & 0 & \cdots & \cdots & 1 & 0 \\ 0 & 0 & 0 & D_{P-2}(\kappa) & -B_{P-1}(\kappa) & 1 \\ 0 & 0 & 0 & 0 & -1 & C_P(\kappa) \end{pmatrix} \tag{86}$$

As before, the topological coefficient κ is calculated from the condition

$$\det \hat{\mathbf{A}}_P = 0$$

Notably, in the case of regular grafting of equally long side chains, $m_i = m$, $n_{ij} = n$, and $q_i = q$, the parameters $B_i = B$, $C_P = C$, and $D_{i-1} = 1$, and matrix $\hat{\mathbf{A}}_P$ reduces to matrix $\mathbf{A}_P$.

Appendix 2: calculation of elastic free energies F_{bb} and F_{sc} for comblike polymer

Elastic free energy F_{bb} of backbone

Distribution of elastic tension in the backbone of comblike polymer (Fig. 5) prompts that the contribution of the side chain in the elastic free energy of comblike polymer is small compared to that of backbone. Using the parabolic potential framework, we estimate in this Appendix the elastic free energy contributions due to the backbone and side chains for a comblike macromolecule with fixed position z_P of its last branching unit.

Similarity between trajectories of the backbone of a comblike polymer and a linear chain with DP M in planar brushes allows us to approximate the relative position z_i/z_P of i-th branching unit as

$$\frac{z_i}{z_P} \approx \sin\left(\frac{\pi i}{2P}\right) \tag{87}$$

and implement the stretching function E_{bb} of the backbone as

$$E_{bb}(z_P, z) = \frac{\pi}{2M}\sqrt{z_P^2 - z^2} \tag{88}$$

In the framework of SS-SCF approach, the elastic free energy of the backbone is then formulated as

$$\frac{F_{bb}}{k_B T} = \frac{3}{2lb}\int_0^{z_P} E_{bb}(z_P, z)\mathrm{d}z = \frac{3\pi^2}{16lb}\frac{z_P^2}{M} \tag{89}$$

Elastic free energy F_{sc} of side chains

$P = M/m$ side chains are exposed to the molecular potential specified by eqn (3) in the main text. The stretching function

$E_{sc,i}$ of the side chain with DP n originating from branching unit i (i = 1, 2,... P) is given by

$$E_{sc,i}(z_i, z) = \kappa\sqrt{\frac{z_i^2}{\cos^2(\kappa n)} - z^2} \tag{90}$$

to give

$$\begin{aligned}\frac{F_{sc,i}}{k_B T} &= \frac{3}{2lb}\int_{z_i}^{z_i/\cos(\kappa n)} E_{sc,i}(z_P, z)\mathrm{d}z \\ &= \frac{3}{4lb}\kappa z_i^2\left[(\kappa n)\left(1 + \tan^2(\kappa n)\right) - \tan(\kappa n)\right] \\ &\approx \frac{z_i^2}{2lbn}(\kappa n)^4, \quad \kappa n \ll 1\end{aligned} \tag{91}$$

The total elastic free energy F_{sc} due to side chains yields

$$\begin{aligned}\frac{F_{sc}}{k_B T} &= q\sum_1^P \frac{F_{sc,i}}{k_B T} \\ &= \frac{z_P^2}{2lbn}(\kappa n)^4 q\sum_{i=1}^{i=P}\frac{z_i^2}{z_P^2} \\ &\approx \frac{z_P^2}{2lbn}(\kappa n)^4 q\sum_{i=1}^{i=P}\sin^2\frac{\pi i}{2P}\end{aligned} \tag{92}$$

By substituting summation by integration,

$$\sum_{i=1}^{i=P}\sin^2\frac{\pi i}{2P} \approx \int_0^P \sin^2\frac{\pi i}{2P}\mathrm{d}i = \frac{P}{2}$$

one finds

$$\frac{F_{sc}}{k_B T} \approx \frac{q}{4lb}\frac{z_P^2}{uM}P^2(\kappa n)^4 \tag{93}$$

where $u = n/m$. By substituting

$$\kappa n = \frac{\pi}{2}\frac{\eta n}{N} = \frac{\pi}{2}\frac{\eta u}{P(1+qu)}, \tag{94}$$

implementing eqn (29) from the main text,

$$\eta = \begin{cases} qP, & P \ll (u/q)^{1/2} \\ (qu)^{1/2}, & P \gg (u/q)^{1/2} \end{cases} \tag{95}$$

and using

$$\eta = (qu)^{1/2}, \quad P \gg (u/q)^{1/2}, \tag{96}$$

the elastic free energy of side chains with $u \gg 1$ is finally evaluated as

$$\frac{F_{sc}(z_P)}{k_B T} \approx \frac{\pi^4}{64lb}\frac{z_P^2}{M}\frac{u}{qP^2} \tag{97}$$

The ratio of the backbone and side chain contributions,

$$\frac{F_{sc}(z_P)}{F_{bb}(z_P)} \approx \frac{\pi^2}{12}\frac{u}{qP^2} \tag{98}$$

indicates that for macromolecules with number of repeats $P \gg (u/q)^{1/2}$, the elastic free energy of side chains is negligible compared with the elastic free energy of the backbone.

Therefore the average elastic free energy of the backbones, $\int_0^H g(z_P)F_{bb}(z_P)\mathrm{d}z_P$, in the brush of comblike polymers will also dominate over the average elastic free energy, $\int_0^H g(z_P)F_{sc}(z_P)\mathrm{d}z_P$, of the side chains.

Acknowledgements

This work was supported by Russian Science Foundation grant 20-13-00270. The authors are thankful to A. A. Darinskii for helpful discussion.

References

1 G. T. Pickett, Classical Path Analysis of end-Grafted Dendrimers: Dendrimer Forest, *Macromolecules*, 2001, **34**, 8784–8791.
2 M. Kröger, O. Peleg and A. Halperin, From Dendrimers to Dendronized Polymers and Forests: Scaling Theory and its Limitations, *Macromolecules*, 2010, **43**, 6213–6224.
3 L. N. Gergidis, A. Kalogirou and C. Vlahos, Dendritic Brushes under Good Solvent Conditions: A Simulation Study, *Langmuir*, 2012, **28**, 17176–17185.
4 A. A. Polotsky, T. Gillich, O. V. Borisov, F. A. M. Leermakers, M. Textor and T. M. Birshtein, Dendritic versus Linear Polymer Brushes: Self-Consistent Field Modelling, Scaling Theory, and Experiment, *Macromolecules*, 2010, **43**, 9555–9566.
5 O. V. Borisov, A. A. Polotsky, O. V. Rud, E. B. Zhulina, F. A. M. Leermakers and T. M. Birshtein, Dendron Brushes and Dendronized Polymers: A Theoretical Outlook, *Soft Matter*, 2014, **10**, 2093–2101.
6 C.-W. Li, H. Merlitz, C.-X. Wu and J.-U. Sommer, The structure of brushes made of dendrimers: Recent Advances, *Polymer*, 2016, **98**, 437–447.
7 F. A. M. Leermakers, E. B. Zhulina and O. V. Borisov, Interaction forces and lubrication of dendronized surfaces, *Curr. Opin. Colloid Interface Sci.*, 2017, **27**, 50–56.
8 F. Wurm and H. Frey, Linear-dendritic block copolymers: the state of the art and exciting perspectives, *Prog. Polym. Sci.*, 2011, **36**, 1–52.
9 E. Blasco, M. Pinol and L. Oriol, Responsive Linear-Dendritic Block Copolymers, *Macromol. Rapid Commun.*, 2014, **35**(12), 1090–1115.
10 H. Garcia-Juan, A. Nogales, E. Blasco, J. C. Martinez, I. Sics, T. A. Ezquerra, M. Pinol and L. Oriol, Self-assembly of thermo and light responsive amphiphilic linear dendritic block copolymers, *Eur. Polym. J.*, 2016, **81**, 621–633.
11 S. Mirsharghi, K. D. Knudsen, S. Bagherifam, B. Niström and U. Boas, Preparation and self-assembly of amphiphilic polylysine dendrons, *New J. Chem.*, 2016, **40**, 3597–3611.
12 X. Fan, Y. Zhao, W. Xu and L. Li, Linear-Dendritic Block Copolymer for Drug and Gene Delivery, *Mater. Sci. Eng., C*, 2016, **62**, 943–959.
13 J. Rzayev, Synthethis of polystyrene-polylactide bottlebrush block copolymers and their melt self-assembly into large domain nanostructures, *Macromolecules*, 2009, **42**, 2135–2141.

14 A. L. Liberman-Martin, C. K. Chu and R. H. Grubbs, Application of Bottlebrush Block Copolymers as Photonic Crystals, *Macromol. Rapid Commun.*, 2017, **38**, 1700058.
15 D. P. Song, T. H. Zhao, G. Guidetti, S. Vignolini and R. M. Parker, Hierarchical Photonic Pigments *via* the Confined Self-Assembly of Bottlebrush Block Copolymers, *ACS Nano*, 2019, **13**, 1764–1771.
16 J. Bolton, T. S. Baile and J. Rzayev, Large pore size nanoporous materials from self-assembly of asymmetric bottlebrush block copolymers, *Nano Lett.*, 2011, **11**, 998–1001.
17 Y. Gai, D.-P. Song, B. M. Yavitt and J. J. Watkins, Polystyrene-*block*-poly(ethylene oxide) Bottlebrush Block Copolymer Morphology Transitions: Influence of Side Chain Length and Volume Fraction, *Macromolecules*, 2017, **50**, 1503–1511.
18 M. B. Runge and N. B. Bowden, Synthesis of High Molecular Weight Comb Block Copolymers and Their Assembly into Ordered Morphologies in the Solid State, *J. Am. Chem. Soc.*, 2007, **129**, 10551–10560.
19 M. B. Runge, C. E. Lipscomb, L. R. Ditzler, M. K. Mahanthappa, A. V. Tivanski and N. B. Bowden, Investigation of the Assembly of Comb Block Copolymers in the Solid State, *Macromolecules*, 2008, **41**, 7687–7694.
20 H.-F. Fei, B. M. Yavitt, X. Hu, G. Kopanati, A. Ribbe and J. J. Watkins, Influence of Molecular Architecture and Chain Flexibility on the Phase Map of Polystyrene-*block*-poly(dimethylsiloxane) Brush Block Copolymers, *Macromolecules*, 2019, **52**, 6449–6457.
21 D. F. Sunday, A. B. Chang, C. D. Liman, E. Gann, D. M. Delongchamp, L. Thomsen, M. W. Matsen, R. H. Grubbs and C. L. Soles, Self-Assembly of ABC Bottlebrush Triblock Terpolymers with Evidence for Looped Backbone Conformations, *Macromolecules*, 2019, **52**(4), 1557–1566.
22 J. Bolton and J. Rzayev, Synthesis and Melt Self-Assembly of PS-PMMA-PLA Triblock Bottlebrush Copolymers, *Macromolecules*, 2014, **47**, 2864–2874.
23 T. Gillich, E. M. Benetti, E. Rakhmatullina, R. Konradi, W. Li, A. Zhang, A. D. Schlüter and M. Textor, Self-Assembly of Focal Point Oligo-Catechol Ethylene Glycol Dendrons on Titanium Oxide Surfaces: Adsorption Kinetics, Surface Characterization, and Nonfouling Properties, *J. Am. Chem. Soc.*, 2011, **133**, 10940–10950.
24 P. Y. J. Yeh, R. K. Kainthan, Y. Zou, M. Chiao and J. N. Kizhakkedathu, Self-assembled monothiol-terminated hyperbranched polyglycerols on a gold surface: a comparative study on the structure, morphology, and protein adsorption characteristics with linear poly(ethylene glycol), *Langmuir*, 2008, **24**, 4907–4916.
25 T. Gillich, C. Acikgöz, L. Isa, A. D. Schlüter, N. D. Spencer and M. Textor, PEG-Stabilized Core-Shell Nanoparticles: Impact of Linear versus Dendritic Polymer Shell Architecture on Colloidal Properties and the Reversibility of Temperature-Induced Aggregation, *ACS Nano*, 2013, **7**, 316–329.
26 M. Vatankhah-Varnosfaderani, A. N. Keith, Y. Cong, H. Liang, M. Rosenthal, M. Sztucki, C. Clair, S. Magonov, D. A. Ivanov, A. V. Dobrynin and S. S. Sheiko, Chameleon-like elastomers with molecularly encoded strain-adaptive stiffening and coloration, *Science*, 2019, **359**, 1509–1513.
27 J. Yuan, A. H. E. Müller, K. Matyjaszewski and S. Sheiko, in *Polymer Science: A Comprehensive Reference*, ed. K. Matyjaszewski and M. Möller, Elsevier, Amsterdam, 2012.
28 S. Tu, C. K. Choudhury, I. Luzinov and O. Kuksenok, Recent advances towards applications of molecular bottlebrushes and their conjugates, *Curr. Opin. Solid State Mater. Sci.*, 2019, **23**, 50–61.
29 G. Xie, M. R. Martinez, M. Olszewski, S. S. Sheiko and K. Matyjaszewski, Molecular Bottlebrushes as Novel Materials, *Biomacromolecules*, 2019, **20**(1), 27–54.
30 A. A. Polotsky, F. A. M. Leermakers, E. B. Zhulina and T. M. Birshtein, On the Two-Population Structure of Brushes Made of Arm-Grafted Polymer Stars, *Macromolecules*, 2012, **45**, 7260–7273.
31 E. B. Zhulina, F. A. M. Leermakers and O. V. Borisov, Theory of brushes formed by Ψ-shaped macromolecules at solid-liquid interfaces, *Langmuir*, 2015, **31**(23), 6514–6522.
32 E. B. Zhulina, F. A. M. Leermakers and O. V. Borisov, Ideal mixing in multicomponent brushes of branched macromolecules, *Macromolecules*, 2015, **48**(23), 5614–5622.
33 I. O. Lebedeva, E. B. Zhulina, F. A. M. Leermakers and O. V. Borisov, Dendron and Hyperbranched Polymer Brushes in Good and Poor Solvents, *Langmuir*, 2017, **33**, 1315–1325.
34 E. B. Zhulina, F. A. M. Leermakers and O. V. Borisov, Brushes of Cycled Macromolecules: Structure and Lubricating Properties, *Macromolecules*, 2016, **49**(22), 8758–8767.
35 E. B. Zhulina, S. S. Sheiko, A. V. Dobrynin and O. V. Borisov, Microphase segregation in the melts of bottlebrush block copolymers, *Macromolecules*, 2020, **53**, 2582–2593.
36 A. N. Semenov, Contribution to the Theory of Microphase Layering in Block-Copolymer Melts, *Sov. Phys. JETP*, 1985, **61**, 733–742.
37 G. J. Fleer, M. A. Cohen Stuart, J. M. H. M. Scheutjens, T. Cosgrove and B. Vincent, *Polymers at Interfaces*, Chapman & Hall, London, 1993.
38 A. E. Levi, J. Lequieu, J. D. Horne, M. W. Bates, J. M. Ren, K. T. Delaney, G. H. Fredrickson and C. M. Bate, Miktoarm Stars *via* Grafting-Through Copolymerization: Self-Assembly and the Star-to-Bottlebrush Transition, *Macromolecules*, 2019, **52**(4), 1794–1802.
39 E. B. Zhulina, S. S. Sheiko and O. V. Borisov, Solution and melts of barbwire bottlebrushes: hierarchical structure and scale-dependent elasticity, *Macromolecules*, 2019, **52**, 1671–1684.
40 E. B. Zhulina, S. S. Sheiko and O. V. Borisov, Planar brush of end-tethered molecular bottle-brushes. Scaling model, *Polym. Sci., Ser. C*, 2018, **60**, 1–8.

